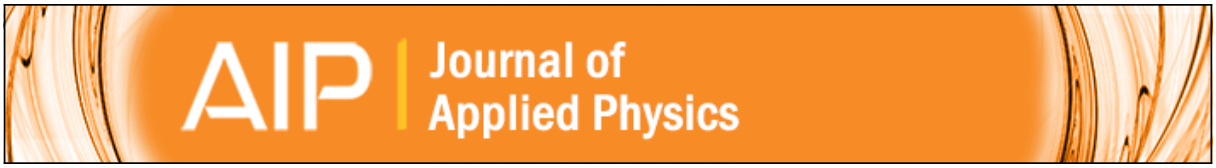

Information dimension analysis of chaotic forward volume spin waves in a yttrium–iron–garnet thin film

A. Prabhakar and D. D. Stancil

Citation: Journal of Applied Physics **87**, 5091 (2000); doi: 10.1063/1.373258
View online: http://dx.doi.org/10.1063/1.373258
View Table of Contents: http://scitation.aip.org/content/aip/journal/jap/87/9?ver=pdfcov
Published by the AIP Publishing

Articles you may be interested in

An antidot array as an edge for total non-reflection of spin waves in yttrium iron garnet films
Appl. Phys. Lett. **104**, 082412 (2014); 10.1063/1.4867026

Single antidot as a passive way to create caustic spin-wave beams in yttrium iron garnet films
Appl. Phys. Lett. **102**, 102409 (2013); 10.1063/1.4795293

Amplification of spin waves in yttrium iron garnet films through the spin Hall effect
Appl. Phys. Lett. **99**, 192511 (2011); 10.1063/1.3660586

Double-wave-front reversal of dipole-exchange spin waves in yttrium-iron garnet films
J. Appl. Phys. **98**, 074908 (2005); 10.1063/1.2077842

Nondispersive magnetostatic forward volume wave propagation in a double-layered yttrium–iron–garnet film structure with dielectric spacer
J. Appl. Phys. **85**, 4862 (1999); 10.1063/1.370046

[This article is copyrighted as indicated in the article. Reuse of AIP content is subject to the terms at: http://scitation.aip.org/termsconditions. Downloaded to] IP: 128.146.58.38 On: Fri, 05 Dec 2014 20:55:31

Information dimension analysis of chaotic forward volume spin waves in a yttrium–iron–garnet thin film

A. Prabhakar[a)]
Read-Rite Corporation, 345 Los Coches Street, Milpitas, California 95035

D. D. Stancil
Department of Electrical and Computer Engineering, Carnegie Mellon University, Pittsburgh, Pennsylvania 15213

Forward volume spin waves were excited in a yttrium–iron–garnet film using a microstrip delay line. Low frequency modulations in output power were captured on a digital oscilloscope for various combinations of microwave input frequency and power. Using the decrease in mutual information as a criterion, an embedding delay time was chosen for each time series. The method of false nearest neighbors was then used to calculate a minimal embedding dimension, D. Despite large changes in input frequency ($4.4\,\mathrm{GHz}<f<4.6\,\mathrm{GHz}$) and power ($15.7\,\mathrm{dBm}<P<22.7\,\mathrm{dBm}$), $D\leqslant 3$ for each time series, indicating a low dimensional system. Finally, the information dimension, d, was estimated by computing the distance from a collection of reference points to their nearest neighbors. The distribution for d was found to be bimodal. When correlated with the input microwave power and frequency, it was found that values of $d<2$ occurred close to the auto-oscillation threshold in the vicinity of an even dipole gap. $d<3$ was observed at higher power levels or at frequencies close to an odd dipole gap. © *2000 American Institute of Physics.* [S0021-8979(00)64608-X]

I. INTRODUCTION

A variety of nonlinear interactions between large amplitude spin waves (SWs) in ferrimagnetic samples are described in the literature.[1–5] Recent investigations of these interactions began with the simplest case of a degenerate SW manifold in spherical samples[6–8] and progressed to studies on nondegenerate manifolds in thin film circular disks.[9] The formation of fingers of auto-oscillation (AO) in the latter experiments was attributed to interactions between a few standing wave modes.[10] Studies on irregularly shaped thin film samples began with observations of a modulational instability for continuous wave excitations[11] and are now focused on investigations of SW soliton formation with pulsed excitations.[12–14] A number of publications also dealt with the collective excitations of the SW manifold above the instability threshold in thin film samples.[15–17]

Experiments were conducted on an irregularly shaped yttrium–iron–garnet (YIG) thin film. Partial pinning of the magnetization on the surfaces of the film lifts the degeneracy among the various propagating SW thickness modes and caused the formation of dipole gaps in the microwave passband.[18,19] The higher energy density in the vicinity of a dipole gap causes the apparent formation of a finger of AO.[20] This phenomenon differs from similar observations of AO in circular thin film YIG resonators where the interactions occur between standing SW modes.[9] We present the results of a dimensional analysis of the output waveform for propagating forward volume SWs over a two-dimensional (2D) phase space consisting of input microwave frequency (f) and power (P). There is evidence to suggest that the instability in a finger depends on whether even or odd thickness modes interact with the predominantly excited zeroth order mode which has even symmetry. Near the AO threshold, nonlinear interactions between modes with like symmetry appear to cause a low dimension instability.

II. EXPERIMENTAL SETUP

The setup used in this experiment was previously used to establish a correlation between fingers of AO and regions with poor microwave transmission characteristics.[20] A low power microwave passband measurement using a network analyzer revealed the existence of dipole gaps caused by the pinning of SW modes on the surfaces of the film. We also observed that the AO threshold was lower in the vicinity of a gap. However, a density plot of the peak-to-peak voltage (V_{pp}) of the output could not differentiate between even and odd numbered dipole gaps. We establish a qualitative difference in AO near even and odd dipole gaps by analyzing the time series output for each combination of P and f.

A schematic of the setup is shown in Fig. 1. The high power microwave passband was measured by sweeping f, feeding the output from the device into a low barrier

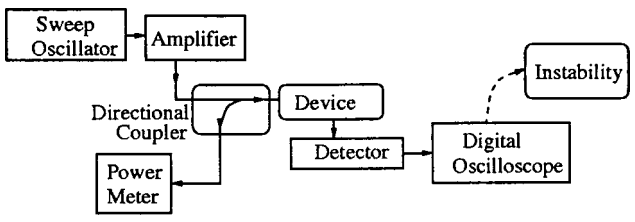

FIG. 1. Experimental configuration used to measure a high power microwave passband by sweeping input frequency or to capture a time series at a constant input frequency and input power. Less than 10% of the power was reflected from the device and picked up by the power meter.

a)Electronic mail: anilpr@yahoo.com

 © 2000 American Institute of Physics
[This article is copyrighted as indicated in the article. Reuse of AIP content is subject to the terms at: http://scitation.aip.org/termsconditions. Downloaded to] IP: 128.146.58.38 On: Fri, 05 Dec 2014 20:55:31

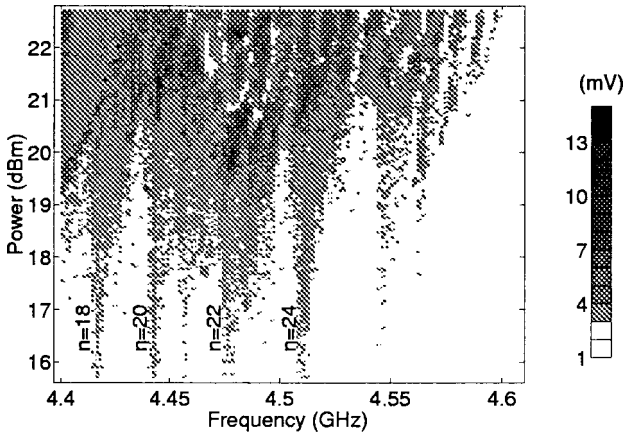

FIG. 2. Density plot of the peak-to-peak voltage of the output from the delay line as measured on the oscilloscope. The locations of the even dipole gaps at low input power are marked on the plot. Weak interactions were visible around 17 dBm near the $n=21$ dipole gap. At higher power levels, fingers of AO corresponding to odd and even dipole gaps merged together.

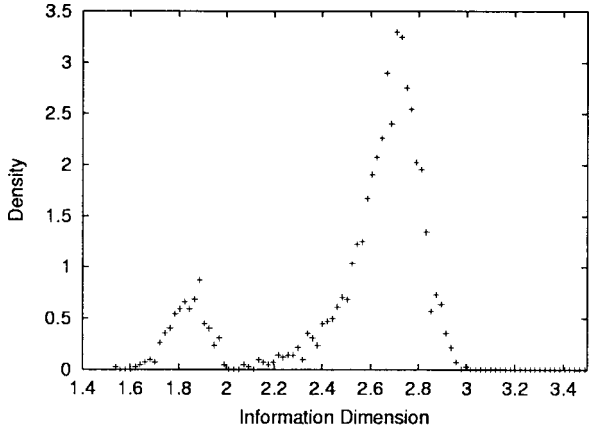

FIG. 3. Histogram of information dimension values, calculated from each chaotic time series as input frequency and power were varied. A total of 2074 data sets were used with 285 sets having $d<2$.

Schottky diode detector (with a 10 MHz–26.5 GHz frequency response) and capturing a trace of the output voltage on a digital oscilloscope. A similar passband was captured at low power using a network analyzer. A comparison between the low and high power passbands allowed us to establish the location and order of the dipole gaps.[20]

In the second stage of the experiment, a continuous wave signal at constant P and f was fed into the device and V_{pp} for the low frequency transmitted signal (<500 MHz) was monitored. Auto-oscillations in the output signal manifest themselves as large values of V_{pp}. Figure 2 is a density plot that shows the variation in V_{pp} as we increment P and f in steps of 0.05 dB and 2 MHz, respectively. A time series snapshot of the output from the detector was captured whenever $V_{pp}>4$ mV. A total of 2074 sets of data were collected. Following a convention where SW mode numbers refer to the number of zeroes in the magnetostatic potential through the thickness of the film, even dipole gaps correspond to interactions between the zeroth order mode and higher order even modes. We observe that nonlinear interactions in the vicinity of an even dipole gap occur at a lower power than in the vicinity of an odd dipole gap. At higher power levels, the even and odd dipole gaps merge to form a single finger of AO.

III. ANALYSIS OF TIME SERIES DATA

The time series data collected when $V_{pp}>4$ mV was analyzed using nonlinear analysis tools which form part of the TISEAN package.[21] An appropriate delay length was determined using a reduction in mutual information as the criterion. The time step where the mutual information dropped to a fifth of its starting value was chosen as the delay length for that particular time series.[22] The minimum embedding dimension, D, was then calculated using the method of false nearest neighbors.[23] While most of the sampled data had $D=3$, for some combinations of f and P the sampled data was well embedded within a 2D space. Since we are dealing with a relatively short time series (4000 points), having a low dimension is highly beneficial. There exist fundamental limitations in numerically estimating the dimension.[24] Eckmann and Ruelle suggest that a maximum number for the dimension is $2\log_{10}N$, where N is the number of data points.[25] Finally, the nearest neighbor information dimension, d, was calculated for each time series using the determined values of delay length and D.[26] The analysis of over 2000 data sets makes the dimensional calculation statistically significant.

A brief description of the nearest neighbor information dimension algorithm is as follows.[27] Given a reference point x on the attractor, one draws k_1 other points at random and without replacement from the attractor. A list of nonnegative distances between x and each of the k_1 points is computed and sorted in increasing order. Fix the order p between 1 and k_1 and let $\delta_p(x,k_1)$ denote the distance between x and its pth nearest neighbor. Then add additional points, again at random and without replacement, to the previous collection for a total of k_2 points and calculate $\delta_p(x,k_2)$. The process continues for an increasing sequence of k_j's until the distance between x and every other point on the attractor has been computed. The entire procedure is repeated for a collection of reference points $\{x_i\}_{i=1}^{R}$ and the mean distance $\langle\delta_p(k)\rangle = \sum_{i=1}^{R}\delta_p(x,k)/R$ is calculated. The nearest neighbor distances scale as $\langle\delta_p(k)\rangle \sim k^{-1/d}$, where d is the information dimension of the attractor. For small data sets, the value obtained for d [by fitting $\log(\langle\delta_p(k)\rangle)$ to a straight line] seemed to depend on our choice of p. However, we observed that d reached an asymptotic value as $p\to 50$. Our focus is on the variation in d with incremental changes in P and f, i.e., between data sets. Using $p=50$ for each data set ensured that the distribution for d over different data sets was unaffected.

Figure 3 is a histogram of d for all the time series sets collected. The bimodal distribution for d reveals a qualitative difference in the nonlinear interactions. The smaller cluster of 285 data sets, with $d<2$, is indicative of low dimension interactions, possibly between two modes. Of interest to us are the combinations of P and f that yield a lower dimension for the output signal. Figure 4 is a bi-level density plot of d over the input space, with the darker shade referring to data sets with $d<2$. By locating the frequencies that correspond to the dipole gaps on this density plot, we observe that the

[This article is copyrighted as indicated in the article. Reuse of AIP content is subject to the terms at: http://scitation.aip.org/termsconditions. Downloaded to] IP: 128.146.58.38 On: Fri, 05 Dec 2014 20:55:31

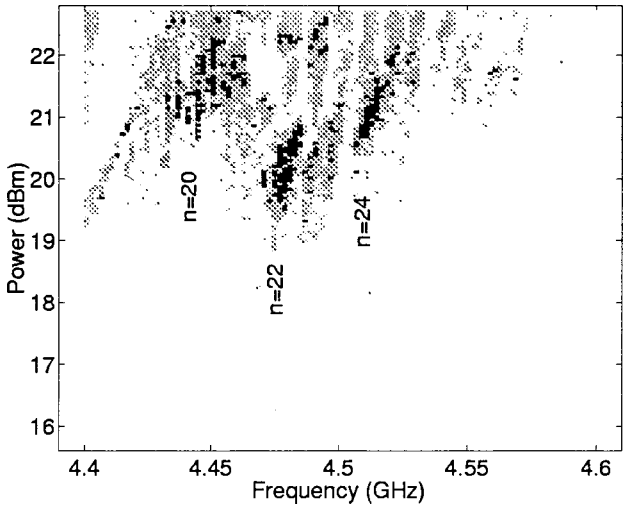

FIG. 4. Bi-level density plot of the information dimension, d, or equivalently a plot of the embedding dimension, D. The dark clusters indicate data sets with $d<2$ and lie close to the location of the even dipole gaps. d increases with an increase in power or a change in frequency.

dark regions lie close to three even numbered dipole gaps. Values of $d>2$ were observed with an increase in P or a change in f and are indicative of more complex interactions between SWs. Since most of the input power is coupled into the zeroth order mode, it is likely that the SW interactions near an even dipole gap have a lower dimension than those at a comparable input power but near an odd dipole gap. However, this difference vanishes with further increases in P.

IV. CONCLUSION

Fingers of auto-oscillation for forward volume spin waves were observed in an irregularly shaped thin YIG film. The frequencies corresponding to the tips of these fingers coincided with the location of dipole gaps in the microwave passband. A large peak-to-peak modulation in the transmitted low frequency microwave signal was indicative of strong auto-oscillations. The output signal was captured as a time series when the low frequency peak-to-peak voltage exceeded a set threshold. Each data set was analyzed to calculate its mutual information, a minimum embedding dimension and a nearest neighbor information dimension. The information dimension distribution was bimodal and its density plot revealed that lower order nonlinear interactions occurred in the vicinity of an even dipole gap. This observation supports the hypothesis that auto-oscillations near an even dipole gap occur largely between the degenerate zeroth order mode and the higher order even SW thickness mode. Higher dimension nonlinear interactions occur at higher power levels or between modes of unlike symmetry.

[1] *Spin Waves and Magnetic Excitations*, edited by A. Borovik-Romanov and S. Sinha (North-Holland Physics, Amsterdam, 1988).
[2] V. S. L'vov, *Turbulence Under Parametric Excitation, Applications to Magnets* (Springer, Berlin, 1994).
[3] *Nonlinear Phenomena and Chaos in Magnetic Materials*, edited by P. Wigen (World Scientific, Singapore, 1994).
[4] *Linear and Nonlinear Spin Waves in Magnetic Films and Superlattices*, edited by M. Cottam (World Scientific, Singapore, 1994).
[5] *High Frequency Processes in Magnetic Materials*, edited by G. Srinivasan and A. Slavin (World Scientific, Singapore, 1995).
[6] G. Gibson and C. Jeffries, Phys. Rev. A **29**, 811 (1984).
[7] P. H. Bryant, C. D. Jeffries, and K. Nakamura, Phys. Rev. A **38**, 4223 (1988).
[8] F. M. Aguiar, A. Azevedo, and S. M. Rezende, J. Appl. Phys. **73**, 6825 (1993).
[9] R. D. McMichael and P. E. Wigen, Phys. Rev. Lett. **64**, 64 (1990).
[10] R. D. McMichael and P. E. Wigen, Phys. Rev. B **42**, 6723 (1990).
[11] B. A. Kalinikos, N. G. Kovshikov, and N. Slavin, JETP Lett. **10**, 392 (1984).
[12] M. A. Tsankov, M. Chen, and C. E. Patton, J. Appl. Phys. **76**, 4274 (1994).
[13] A. N. Slavin, Phys. Rev. Lett. **77**, 4644 (1996).
[14] R. A. Stuadinger *et al.*, IEEE Trans. Magn. **34**, 2334 (1998).
[15] X. Y. Zhang and H. Suhl, Phys. Rev. B **38**, 4893 (1988).
[16] V. B. Cherepanov and A. N. Slavin, J. Appl. Phys. **73**, 6811 (1993).
[17] V. B. Cherepanov and A. N. Slavin, Phys. Rev. B **47**, 5874 (1993).
[18] T. Wolfram and R. E. DeWames, Phys. Rev. B **4**, 3125 (1971).
[19] B. Kalinikos and A. N. Slavin, J. Phys. C **19**, 7013 (1986).
[20] A. Prabhakar and D. D. Stancil, Phys. Rev. B **57**, 11483 (1998).
[21] R. Hegger and H. Kantz, Chaos **9**, 413 (1999).
[22] H. D. I. Abarbanel, R. Brown, J. J. Sidorowich, and L. S. Tsimring, Rev. Mod. Phys. **65**, 1331 (1993).
[23] M. Kennel, R. Brown, and H. D. I. Abarbanel, Phys. Rev. A **45**, 3403 (1992).
[24] E. J. Kostelich and H. L. Swinney, in *Chaos and Related Nonlinear Phenomena*, edited by I. Procaccia and M. Shapiro (Plenum, New York, 1987).
[25] J. P. Eckmann and D. Ruelle, Physica D **56**, 185 (1992).
[26] R. Badii and A. Politi, J. Stat. Phys. **40**, 725 (1985).
[27] E. J. Kostelich (unpublished).

[This article is copyrighted as indicated in the article. Reuse of AIP content is subject to the terms at: http://scitation.aip.org/termsconditions. Downloaded to] IP: 128.146.58.38 On: Fri, 05 Dec 2014 20:55:31